Available online at www.sciencedirect.com
SCIENCE DIRECT®
PERGAMON
International Journal of Heat and Mass Transfer 46 (2003) 4245–4256
International Journal of HEAT and MASS TRANSFER
www.elsevier.com/locate/ijhmt

Boiling incipience of highly wetting liquids in horizontal confined space

V. Dupont *, M. Miscevic, J.L. Joly, V. Platel

Laboratoire d'Energétique, Université Paul Sabatier, 118 route de Narbonne, 31062 Toulouse, France

Received 30 May 2002; received in revised form 14 April 2003

Abstract

This study concerns boiling incipience of highly wetting liquids (*n*-pentane), in transient conditions, in horizontal confined space between a vertical heating cylinder and a disk. The two controlled parameters were the heat flux, ranging from 50 to 200 kW m^{-2} and the thickness of the liquid in the confined space, ranging from 0 to 240 μm. Experiments were conducted with both smooth and porous disks. The results suggest that in the porous-disk configuration, boiling could appear on the non-heated wall.

1. Introduction

In the last decades, the miniaturization of electronics devices and the continuous increases of the electrical power for such devices involve a significant rise in the heat flux to be dissipated. This evolution has induced an important effort to miniaturize the heat exchangers, to match the scale of these microsystems or to reduce the size and the weight of existing devices. This trend is particularly sensitive in spatial inboard equipment where two-phase exchangers offer a good stability and homogeneity of temperatures with high heat transfer performances.

Unfortunately, the working fluids used in these applications (ammonia, FC-72, FC-76, R-134a) have been found to display highly wetting behavior on widely used materials. The large boiling incipience superheat excursion, associated with highly wetting liquids, could produce thermomechanical stress and aging on the boiling surface that might reduce, for example, the lifetime and the efficiency of the electronical chip. This problem has been the subject of a large amount of research.

In space applications, where efficient and reliable thermal management systems are needed, the interest in boiling incipience in confined space is linked to the startup phase of a capillary pumped loop [1–3]. In the evaporator of such devices, in fully flooded conditions, boiling starts in a space located between the heated body of the evaporator and a porous wick saturated with liquid. This configuration could be encountered in other applications, such as wick heat pipes, microheat exchangers and in systems related with phase change in porous media.

The first work on boiling incipience was performed in the 50's by Corty and Foust, Bankoff et al. [4] and have allowed us to understand the main mechanisms and to evaluate the critical liquid superheat related to the creation of the vapor phase near a heated wall. Bar-Cohen and Simon [5] have done a brief review of the mechanisms, influential parameters and limited literature on incipience superheat excursions in the case of highly wetting liquids. The authors defined superheat excursion as the difference between the superheat required to activate embryonic vapor bubbles and the superheat necessary to sustain nucleate boiling. They pointed out the difficulties to predict this excursion.

Tong et al. [6] analyzed the influence of the dynamic solid/liquid contact angle and contact angle hysteresis

* Corresponding author. Address: Laboratoire de Transfert de Chaleur et de Masse, Swiss Federal Institute of Technology, CH-1015 Lausanne, Switzerland. Tel.: +41-21-693-54-41; fax: +41-21-693-59-60.

E-mail address: vincent.dupont@epfl.ch (V. Dupont).

0017-9310/$ - see front matter © 2003 Elsevier Ltd. All rights reserved.
doi:10.1016/S0017-9310(03)00268-0

Nomenclature

a	thermal diffusivity [m^{-2} s]
C_p	specific heat [J kg^{-1} K^{-1}]
e	confinement height [m]
L	cylinder height [m]
L_v	latent heat of vaporization [J kg^{-1}]
q_0	heat flux [W m^{-2}]
r	radius (pore or bubble) [m]
T	temperature [K]
P	pressure [Pa]
ΔP	differential pressure [Pa]
R_a	averaged roughness [m]
V	volume [m^3]
W_t	waviness height [m]
t	time [s]

Greek symbols

α	thermal dilatation coefficient [K^{-1}]
ΔT	temperature difference [K]
ε	porosity [ ]
λ	thermal conductivity [W m^{-1} K^{-1}]
σ	surface tension [N m^{-1}]
ρ	density [kg m^{-3}]

Subscripts

b	bubble
bi	boiling incipience
c	critical
cyl	cylinder
i	incipience
mnsc	liquid meniscus
l	liquid
p	pore
prs	porous
sat	saturation
thr	threshold
v	vapor
w	wall

on the boiling incipience superheat of highly wetting liquids. This analytical work was based on a modified Lorenz model with assumption of the conservation of the trapped vapor volume according with the Bankoff criteria [4]. Assuming a conical shape for the cavity, the mouth radius corresponds to the maximum radius of the cross-section of this cavity. The bubble critical radius value in the case of highly wetting liquids has been shown to lie below the mouth radius value of the active cavity. The dynamic contact angle is dependent on the velocity of the three-phase line. Then the critical radius depends on the trapping interface velocity and the filling conditions. The critical bubble sizes are compatible with the dimensions of the cracks and holes present on the boiling surfaces.

You et al. [7,8] conducted FC-72 and R-113 saturated pool boiling experiments at atmospheric pressure, using a 0.13 mm diameter chromel wire and 0.51 mm diameter platinum cylinder, as heater surfaces, or 0.5 μm films of silicon, silicon dioxide and aluminum oxide. To take into account the scattered behavior of the phenomena, the authors defined a "boiling incipience probability". For R-113, the incipience superheat ranged from 43 to 75 °C, and for FC-72 from 18 to 51 °C. The properties of the liquid affects wall superheat values but the material effect was less significant than the surface microgeometry for highly wetting dielectric fluids. The capacity of such fluids to flood microcavities induces large superheats at incipience. The authors showed the necessity to take into account the non-linearity of the saturation curve and the surface tension temperature dependence in superheat evaluation.

With dielectric fluids, superheat excursions may be encountered on smooth as well as on enhanced surfaces. Incipience behavior on enhanced surfaces with porous coatings depends on the microgeometry of the porous material. Bar-Cohen and Simon [5], Bergles [9], Afgan et al. [10] showed that $\Delta T_{sat\,i}$ decreases with porous coating compared to a smooth surface, but the boiling excursion remains constant due to the improvement of the heat transfer coefficient. Tevher et al. [11] observed an opposite behavior on tubes with porous metallic coating with R-113 as working fluid. Chang et al. [12] conducted an experimental study on incipience boiling with a copper plate covered by a "microporous" or "porous" coating, with a thickness ranging from 30 to 250 μm, in a FC-72 pool. The coating was constituted by resin and diamond particles. The particle diameters ranging from 0 (plain surface) to 70 μm. Results showed that as the particle size increases, the mean incipience boiling superheat decreases significantly (by a factor 6) and reach a limit value beyond a diameter of 20 μm. If the particles in the coating are too large the cavities are flooded by the liquid. If the particles are too small the existing cavities give large boiling incipience superheats. Liang and Yang [13,14] illustrated the fundamental importance of the contact angle comparing boiling incipience of *n*-pentane on a flat copper surface and on a porous graphite–copper composite surface. The use of micro-graphite–copper fiber reduced considerably the hysteresis at boiling incipience, by increasing the number

and the size of the nucleation sites and its capacity to preserve the vapor nucleus. The authors explained these results by considerations on the contact angle: ~2° for the *n*-pentane on copper versus ~35° for the *n*-pentane on graphite.

Research on boiling incipience in confined space has been rarely discussed in literature. Thome [15] reported that placing a smooth glass or stainless steel ball in the bottom of a smooth beaker filled with small superheated ($\Delta T_{\text{sat}\,i} = 0.1$ °C) double-distilled and well-boiled water, makes boiling initiate. When the glass ball is removed from the surface, boiling ceases. The author concluded that the trapping mechanism of boiling nucleation theory does not seem to explain these results. Reed and Mudawar [16] examined the effects on $\Delta T_{\text{sat}\,i}$ of the contact forces and material conductivity on a heated vertical wall in contact with single or multiple spherical points, with FC-72 as test fluid. Contact pressure has small influence on boiling incipience. The nature of the sphere material was important: for solid copper, $\Delta T_{\text{sat}\,i}$ increases because of the thermal dissipation (fin effect). In the case of aluminum capped Lexan spheres, a decrease in ΔT_{sat}, was observed due to a local hot point located at the contact area.

1.1. Study objectives

The aim of this study was to understand the main mechanisms related to boiling incipience from a pre-existing vapor nucleus, in the transient state, inside a superheated liquid layer located between an heated wall and a porous-disk saturated with liquid, after the application of a power step. The effects of the confinement height, heat flux, and surface microgeometry were investigated.

2. Experimental apparatus and procedure

2.1. Experimental apparatus

The experimental set-up shown in Fig. 1 was inspired from the Liang and Yang [14] device. The main features were the enclosure filled with *n*-pentane, the displacement system of the heated surface, the liquid level control vessel, the condenser and the data acquisition system.

The enclosure was made in AG3 (inner volume: $190 \times 190 \times 260$ mm) equipped with two transparent PVC windows. The operating temperature was fixed by water circulation, inside two lateral walls and the floor of the enclosure. The temperature of the water was fixed by a thermostat-controlled bath with an accuracy of 0.1 °C. The liquid level was one-fourth of the total height and could vary (±5 mm) by vertical displacement of a V-shaped vessel. The test with *n*-pentane were at a saturation temperature of 36.2 °C at 1 atm. Two K-type thermocouples were placed in the bath and the vapor allowing to control the saturation conditions.

Fig. 2 shows the confinement control system. The height of the liquid between the heated cylinder and the fixed disk was called confinement height *e*. The heated cylinder (30 mm diameter and 14.8 mm height) shown in Fig. 3 was made in AU4G, and fixed on a vertical displacement stage controlled by a micrometric-screw. The height *e* of the confined space was controlled from outside the enclosure, in the range from 0 (contact) to 2000 μm. The upper surface of the cylinder was in close contact with a heating element (a metallic foil embedded in a mica layer), and with the PTFE insulation. This heating element provided a uniform heat flux to the upper surface of the heating cylinder. The lower surface

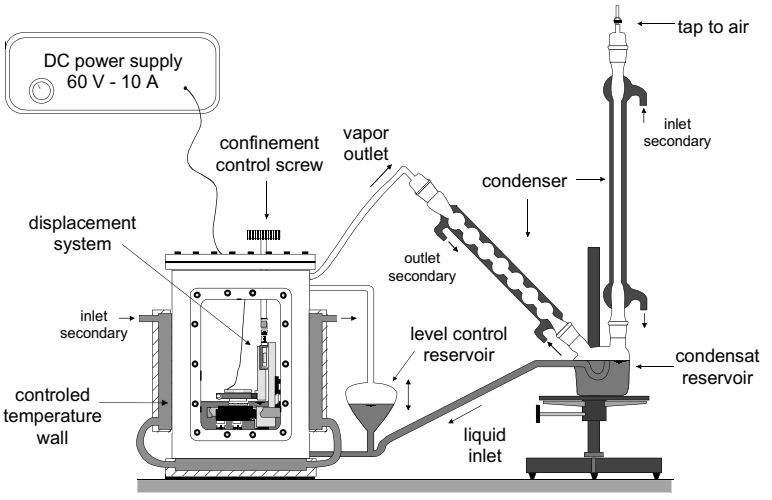

Fig. 1. Confinement boiling test facility.

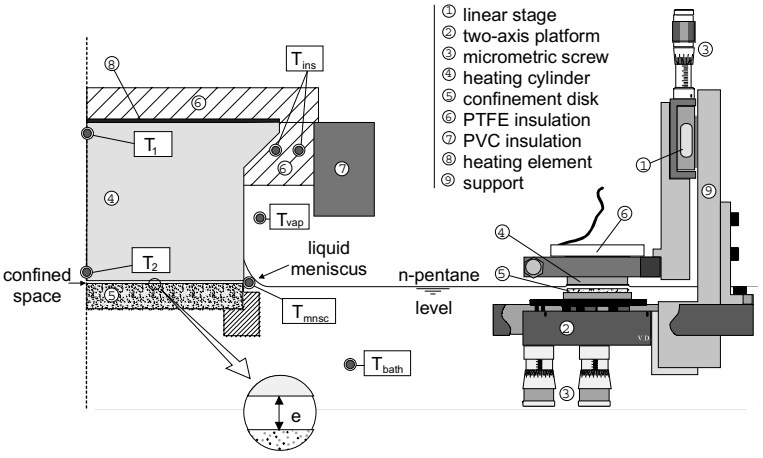

Fig. 2. Displacement system (right) and half-test section.

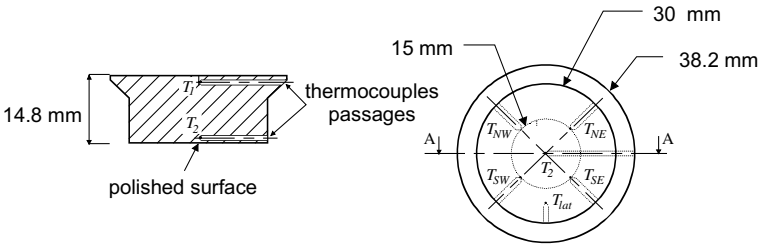

Fig. 3. Thermocouples positions in the heated cylinder.

was mechanically polished until a mirror aspect was obtained, using successively 300, 400, 600, 800 grades sand paper and 8, 4, 2 and 1 μm diamond powder. This procedure was applied in order to control the surface state and to obtain high incipience boiling superheats. A good flatness was obtained by crossing the polish direction between each level and polishing the cylinder inside a ring. The mean wave height and roughness were respectively $W_t = 6$ μm and $R_a = 0.067 \pm 0.01$ μm. These values were measured with a needle rugosimeter on the polishing ring. Measurement with an interferometric rugosimeter gave $R_a = 0.018$ μm directly on the polished face and values of R_a ranging from 0.75 to 0.88 μm on the lateral raw surface of the cylinder.

The heating cylinder was instrumented with seven K-type thermocouples, 0.5 mm diameter, located at 0.8 mm from the lower and upper surface as represented in Fig. 3. The radial path of the thermocouples followed the isothermal plane and the external space between thermocouple sheaths and the borings were sealed to avoid liquid penetration.

Plain and porous Pyrex 30-mm diameter disks were tested. In the case of the smooth glass disk, its surface state was characterized by $W_t = 0.07$ μm and $R_a = 0.042 \pm 0.01$ μm. The porous disk was more difficult to polish; a privileged flat contact area was formed at the center of the disk. The washing process, to open the pores after polishing, was previously described by Faghri [17]. The disk was passed in an ultrasonic bath with successively, acetone, ethanol and distillated water. It was then dried in an oven, at 80 °C for 6 h, and placed in a vacuum enclosure to 10^{-4} Torr and finally saturated with *n*-pentane. MEB view (Fig. 4) of the porous disk before and after the washing had validated this process. The structure of the porous media was an ovoid particle stacking. A mercury porosimeter evaluation indicated a porosity of $\varepsilon = 0.36$ and pore diameters ranging from 1.8 to 51.5 μm with a mean value of 17 μm.

The determination of the boiling incipience instant is very difficult to obtain by placing a sensor in the confined space. Such a sensor could modify the conditions necessary to onset the nucleate boiling. Thus, two thermocouples, T_{mnsc1} and T_{mnsc2}, were placed diametrically opposite inside the liquid meniscus, in front of the confined space. There were no direct contact between the head of the thermocouples and the cylinder or the confinement disk. The role of these sensors was fundamental in the determination of the instant of boiling incipience.

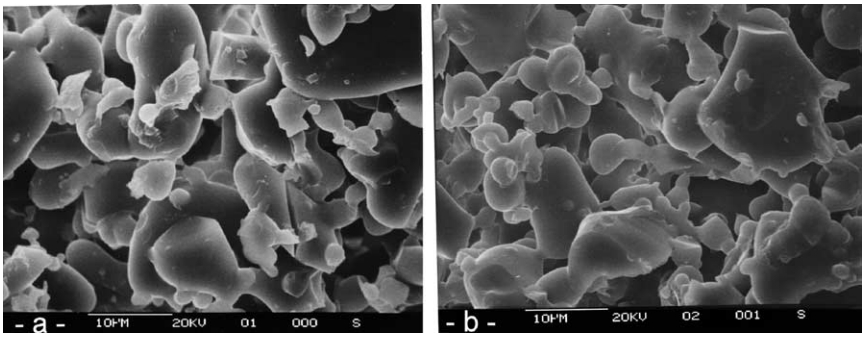

Fig. 4. SEM view of porous confinement disk, before (a) and after the washing process (b).

A PC acquisition card (National instrument system with SCXI-1303 module) was used to read and store data. The K-type thermocouples had a diameter of 0.5 mm with the soldering directly in contact with the Inconel sheath. The response time of these thermocouples in the liquid was evaluated to be less than 0.1 s. All the thermocouples were calibrated using a platinum resistance thermometer. Uncertainty on temperature measurement was estimated to be within 0.2 °C. Acquisition has been done at 10 Hz: 100 samples/s with a mean value on 10 samples. A video camera and a S-VHS video tape recorder were used for detecting, by visualization, the incoming of the first bubble. The heat flux q_0 was equal to the electric power supplied divided by the test section area. Uncertainty on power supplied was 10.1% at 50 kW m^{-2} and 6.3% at 200 kW m^{-2}.

2.2. Narrow space thickness adjustment

The porous (or smooth) disk was fixed on a two-axis platform. Parallelism of the confined space was controlled by two micrometric screws using a shadowgraphy method. The uncertainty on parallelism was ±10 μm on the vertical. The wavy aspect of the surfaces created privileged contact points when $e = 0$ μm. The main difficulty was the "zero" determination on the micrometric screw scale when the surfaces were in contact. This reference point was determined by the disengaging of the micrometric screw and the resulting uncertainty, constant for a given cylinder-disk configuration, was one graduation (±20 μm). The length of stroke of the vertical displacement stage was less than 1 μm.

An another source of uncertainties was the thermal dilatation of the cylinder (AU4G, $\alpha = 22 \times 10^{-6}$ K^{-1}) during the transient phase: $\Delta L = \alpha \Delta T L$. The resulting uncertainty on thickness value of the confined space was $\Delta e = 4.9$ μm for $e = 0$ μm ($\Delta T = 15$ °C), $\Delta e = 11.4$ μm for $e = 200$ μm ($\Delta T = 35$ °C). Neglecting the part of error due to displacement stage sensibility, in the most unfavorable case, uncertainties on confinement values were, at the limits of the range, $e = 0 \pm 24.9$ and 200 ± 31.4 μm.

2.3. Test procedure

The inside wall of the box was carefully washed, in an ultrasonic bath for the small pieces. Bar-Cohen and Simon [5] have shown the ability of liquids as R-113 or FC-72 to dissolve an important quantity of air. These dissolved gases lowered $\Delta T_{\mathrm{sat}\,i}$ and increased the discrepancy of the results. You et al. [18] demonstrated that violent boiling is effective to degas efficiently a wall. Consequently, the following procedure was adopted; before a series of tests, enclosure and cylinder were heated for a half-hour to generate intensive boiling in the bath. Saturation conditions in the enclosure were controlled.

Another difficulty was the "aging" process, the microgeometry of the boiling surface could oxize, chemical deposits could appear, etc. Liang and Yang [13], evoking this problem, polished their surface between two tests. In our case, the method of You et al. [8] consisting of waiting for the surface stabilization was chosen. We conducted aging studies based on several hundred boiling incipience on the cylinder alone. As a result of these studies, each new cylinder used was heated during 2 h in order to obtain an intense boiling on the bottom surface. The early phase of the aging process was thus accelerated and a stable behavior was obtained afterward.

After the degassing process, each series of tests followed the same procedure. The level of *n*-pentane in the pool was adjusted to permit the wetting of the confinement zone and avoid lateral boiling on the cylinder (1 mm height meniscus). After the confinement height setting, a heat flux step was applied at the top of the cylinder until boiling incipience was observed. The power was then shut down a severals seconds after. The time separating the two tests ranged from 10 to 20 min, depending on the former boiling incipience superheat value.

The procedure to determine the cylinder superheat ($T_{\mathrm{cyl}} - T_{\mathrm{sat}}$) at boiling incipience is the following:

1. at the point in time where there is a sudden change in temperature of the two thermocouples placed in the liquid meniscus, the time corresponding to the appearance of a bubble is determined,
2. the video is used to confirm that the bubble is the first and comes from the confined space and not from the top of the lateral meniscus,
3. the mean temperatures of the cylinder (at 0.8 mm from the surface), corresponding to this boiling time are noted. This temperature is not used to detect incipience in the confined space.

The bubble grows in the superheated liquid layer in the confinement. Moriyama and Inoue [19] have measured the velocity of the front of a bubble growing in a superheated R-113 in a similarly confined space (e ranging from 100 to 400 μm). The velocity ranged from 0.5 to 4 m/s. Using this order of magnitude in our device the characteristic time associated with the exit of the bubble from the confined space ranges from 3.75 to 30 ms. These values are one or two order of magnitudes lower than the acquisition rate (0.1 s). Thus bubbles appear always between two acquisitions: there is no delay due to the displacement of the bubble (of n acquisitions) to take into account in the determination of the instant of boiling in the confinement. The exit is violent, sometimes with an audible noise, and the impact on the free surface is clearly visible with the camera (mechanical effect) and with the sudden variation on the temperature of two thermocouples placed in the meniscus (thermal effect). "Hidden" boiling is not possible in the confined space because of this violent growing of the bubbles.

Due to the scattered behavior of boiling incipience phenomena, at least five measurements were made for each experimental set of parameters (e, q_0). The tests were performed with confined space heights ranging from 0 to 200 μm, and with heat flux ranging from 50 to 200 $\mathrm{kW\,m^{-2}}$.

3. Experimental results

Results presented here concern boiling incipience tests performed with a plain Pyrex disk and a porous Pyrex disk. For each case, particular attention was paid on temporal evolution analysis and a synthesis was proposed. Finally, these experimental results are discussed.

3.1. Plain disk configuration

Fig. 5a shows the temperature history of the system after the application of a heat flux $q_0 = 200\ \mathrm{kW\,m^{-2}}$, at $t = 5$ s, for $e = 60$ μm. This test was representative of the behavior of the system in the plain-disk configuration. Conductive heat transfer, from the top surface, increases the cylinder temperature (the six thermocouples placed near the confinement surface have a nearly identical evolution). Evolutions of T_{mnsc1} and T_{mnsc2} (right scale), placed in the liquid meniscus around the cylinder perimeter, have a fluctuation due to complex heat and mass transfer in this area.

At $t_{\mathrm{bi1}} = 18.4$ s (area A), for $\Delta T_{\mathrm{sat}\,i} = 10.9$ °C, boiling appears in the meniscus on the side of the cylinder as confirmed by video analysis. Phase change and mixing effect of boiling involve a fall in T_{mnsc} evolution. Before t_{bi1} the variation in time of the six temperatures at 0.8 mm from the surface were superposed. After, the boiling in the meniscus increased the heat transfer at the periphery and created a radial gradient of temperature in the cylinder that entails a dispersion in the time variation of the temperatures. At low heat flux (or if the liquid level is too high), a steady state is reached. This "parasite" boiling incipience, out of the area of interest, determines the minimum value of the heat flux studied ($q_0 > 50\ \mathrm{kW\,m^{-2}}$). At higher heat flux, as the case of Fig. 5a, lateral heat transfer was not sufficient to evacuate all the heat from the cylinder and the temperatures still grow. At $t_{\mathrm{bi2}} = 30.5$ s (area B), for $\Delta T_{\mathrm{sat}\,i} = 25.3$ °C, boiling appears suddenly, with a detonation, involving a break in the T_{cyl} slope and totally drying the confined space. Then, the cylinder temperature increased dramatically and the power supply was stopped approximatively 7 s after t_{bi2} (top of the T_{l} curve). Fig. 5b resumes this double boiling incipience scenario. A schematic representation of the various zones where boiling appears is also illustrated.

The $\Delta T_{\mathrm{sat}\,i}$ presented in this study were the differences between T_{cyl} (the mean value of the six temperatures near the surface: T_2, T_{lat}, T_{NW}, T_{NE}, T_{SW}, T_{SE}) and the saturation temperature at t_{bi1} or t_{bi2}. The uncertainty on t_{bi1} leads to $\Delta T_{\mathrm{sat}\,i}$ values within ±1.5 °C in the worst case. This poor accuracy was not penalizing because this boiling occurs out of the interest area. It was interesting to evaluate the order of magnitude of $\Delta T_{\mathrm{sat}\,i}$ in this case. The determination of t_{bi2} was more accurate and uncertainty on $\Delta T_{\mathrm{sat}\,i}$ was of the same order of magnitude than the thermocouple precision. Moreover, some numerical simulations have been performed in order to compare T_{surface} and T_{cyl} at the boiling incipience instant [20]. The model is presented in Appendix A. These simulations have shown that the difference between this two temperatures was ranging from 0.02 to 0.1 K for a heat flux ranging from 5 to 20 $\mathrm{kW\,m^2}$. The order of magnitude of $T_{\mathrm{surface}} - T_{\mathrm{cyl}}$ was then nearly the same than the temperature uncertainties and thus no correction was performed.

Fig. 6 represents $\Delta T_{\mathrm{sat}\,i}$ versus the height of the confined zone with four heat flux values. Results of 131 incipience tests are reported. Each represented point was the mean value of, at least, five tests and error bars were

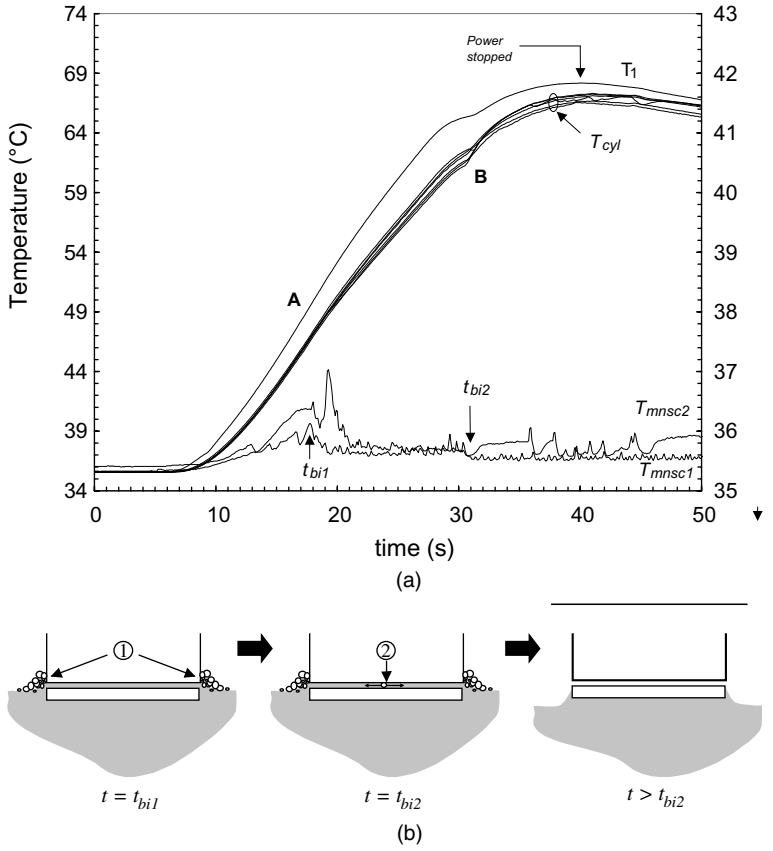

Fig. 5. Heated cylinder and meniscus temperature versus time in the flat-disk configuration, $q_0 = 200\ \mathrm{kW\,m^{-2}}$, $e = 60\ \mu\mathrm{m}$ (a) and double boiling incipience in the flat-disk configuration (b).

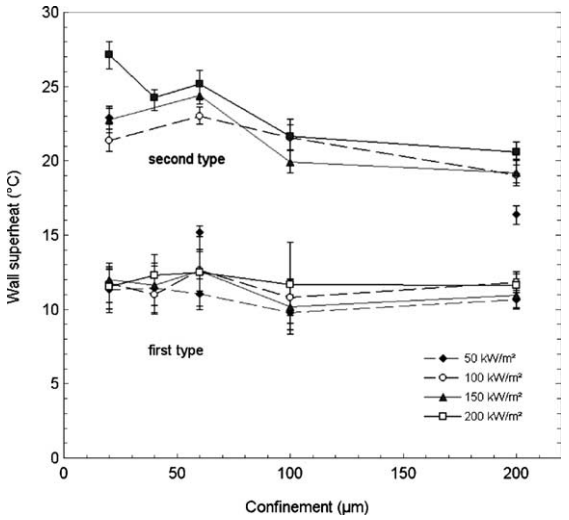

Fig. 6. $\Delta T_{\mathrm{sat}\,i}$ versus thickness of the confined space value with different heat flux, in the plain-disk configuration.

the 95% confidence interval calculated using the appropriate value of Student's multiplier which take into account the number of degrees of freedom of the dataset [21]. The two types of boiling incipience were observed. For the first type i.e. side cylinder boiling incipience, the mean superheat was quite stable, ranging from 10.7 to 15.2 °C, corresponding to the observed superheat values of the cylinder alone during aging tests. For the second type i.e. boiling on the polished surface, the mean superheats were larger, ranging from 16.4 to 27.2 °C and decrease with e. At this time no clear explanation is proposed to this decrease. This two superheat deviation was correlated to the difference of the surface state between the lateral wall and the bottom surface of the cylinder. The existing sizes of sites present on the polished surface were small and less numerous than on the raw lateral surface.

3.2. Porous disk configuration

Fig. 7 shows the evolution of the temperature of the heated cylinder with a heat flux step value of

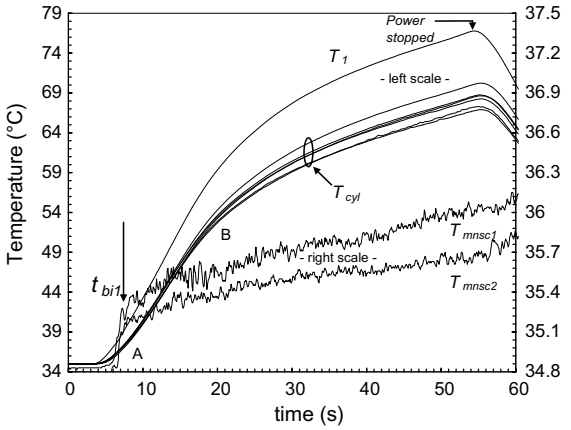

Fig. 7. Heated cylinder and meniscus temperature evolution in the porous-disk configuration, $q_0 = 200$ kW m^{-2}, $e = 60$ μm.

200 kW m^{-2} and $e = 60$ μm. The only difference with the results presented in Fig. 5 was the nature of the confinement disk, porous here. At $t_{bi1} = 6.8$ s (area A), for $\Delta T_{sat\,i} = 0.9$ °C, evolution of T_{mnsc1} and T_{mnsc2} (right scale) exhibited sudden variations: bubbles appeared in the confined zone, involving a light diverging evolution of surface temperatures. Video observations agreed with this interpretation.

This type of boiling incipience occurs with a superheat one order of magnitude lower than in the plain-disk configuration. This fundamental behavior difference is only determinated by the nature of the surface state of the confinement disk. For small spacings, when the disk is a porous medium, heat transfer through the liquid layer allows the fluid to reach boiling conditions on the porous top surface, before the boiling incipience superheat was reached on the polished surface. In brief, boiling can appear elsewhere than on the heated surface.

Heat transfer, after this first boiling incipience, was limited, and the cylinder temperature still grows until boiling appears on the lateral wall, for $\Delta T_{sat\,i} \approx 13$ °C, involving a slope change (area B).

With a 200 μm thickness value, the behavior related to boiling incipience was nearly the same as that for the plain-disk configuration (Fig. 5). When the spacing is too important, the surface state of the disk has no effect; first, boiling takes place in the meniscus, and then on the polished surface with a detonation. Fig. 8 summarizes, ordered by increasing superheat level, the three places where boiling could appear in the porous-disk configuration.

Height value of the narrow space has a strong influence on boiling superheat value for the porous-disk configuration, independently of the value of q_0:

$e < 100$ μm: $0.6 \leqslant \Delta T_{sat\,i} \leqslant 3.5$ °C

$e > 180$ μm: $17.5 \leqslant \Delta T_{sat\,i} \leqslant 25.3$ °C

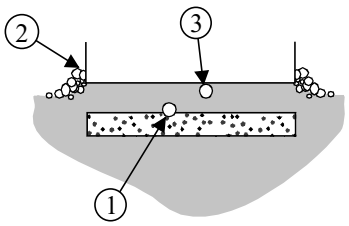

Fig. 8. Three types of boiling incipience in the porous-disk configuration.

These two ranges of superheat correspond respectively to boiling incipience on the porous surface and on the polished surface. Between these two values, there was a transition range of heights where boiling could appear, randomly, at any of the three locations defined in Fig. 8. The width of this transition range varies with q_0. Based on the knowledge on the previous superheat determination with the plain-disk configuration, for each test, mean $\Delta T_{sat\,i}$ have been classified in one of the three following groups (different from the "types" of Section 3.1):

Group 1: porous $\Delta T_{sat\,i} < 10$ °C
Group 2: meniscus 10 K $\leqslant \Delta T_{sat\,i} \leqslant 16$ °C
Group 3: polished surface 16K $< \Delta T_{sat\,i}$

Fig. 9 presents mean $\Delta T_{sat\,i}$ versus height, measured for groups 1 and 3 (the few points of group 2 are omitted), for four heat flux values. In the transition range, for a given set of parameters (e, q_0) two values of mean boiling incipience superheat were possible. For example, with

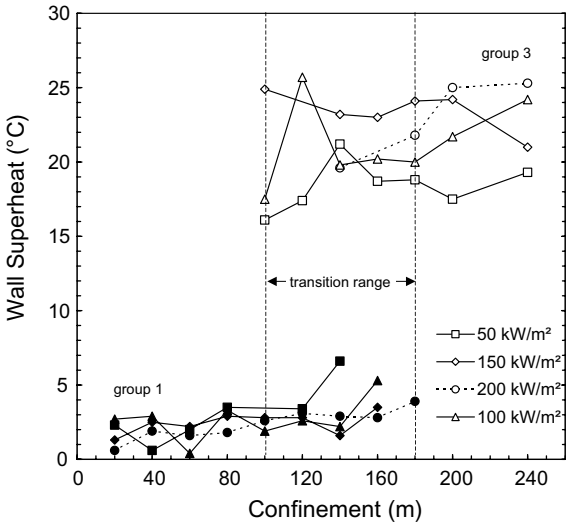

Fig. 9. Mean boiling incipience superheat versus confinement value, with different heat flux.

$q_0 = 150$ kW m^{-2} and $e = 140$ μm, for group 1, $\Delta T_{\text{sat}\,i} = 2.9$ °C and for group 3 $\Delta T_{\text{sat}\,i} = 23.2$ °C. The existence of this transition area was due to the natural discrepancies of boiling incipience superheat for both surfaces delimiting the confined zone.

4. Growing criteria and first bubbles localization

Previous experimental results showed that, in a liquid layer delimited by a wall heated in a transient way and non-heated wall, boiling could appear, in certain cases, on the thermally inert surface. This phenomenon was controlled by the difference of the superheat values necessary to initiate boiling on both surfaces and by heat transfer through the superheated liquid layer. On the polished surface, $16.1 \leqslant \Delta T_{\text{sat}\,i} \leqslant 27.2$ °C; when boiling starts on the porous disk, the mean wall superheat values of the cylinder was ranging from 0.4 to 6.6 °C. This range implied small values of boiling incipience superheat on the porous structure.

4.1. Critical bubble radius evaluation

It is commonly accepted that three types of boiling incipience could be encountered. The first, homogeneous boiling, occurs inside pure highly superheated liquid where clusters of molecules with significant energies can act as bubble nuclei [22,23]. The second, heterogeneous boiling, occurs in the presence of a solid wall. In this case, considering the same liquid superheat, a contact angle between the liquid vapor interface and the wall exists. This contact angle lowers the volume and surface needed to create the vapor bubble (or truncated bubble in this case) and so lowers the energy necessary for vaporization [24] i.e. poorly wetting fluids exhibit lower boiling incipience superheat than highly wetting fluids. The third type, i.e. nucleate boiling, is initiated from the activation process of preexisting vapor nuclei trapped in surface cavities of the wall. All the physical models of boiling initiating are based on the assumptions of mechanical, chemical and thermal equilibrium between vapor and liquid phases during the bubble growth. The interface position inside the cavity is determined by two parameters: contact angle (at the three-phase line) and the liquid superheat which fixes the interface curvature at equilibrium. Using Clapeyron and Laplace equations and assuming that the specific volume of the liquid is negligible compared to the specific volume of the vapor [7]:

$$\Delta T_{\text{sat}\,i} = T_{\text{w}} - T_{\text{sat}}(P_{\text{l}}) \simeq \frac{2\sigma}{r_{\text{c}}} \frac{T_{\text{sat}}(P_{\text{l}})}{\rho_{\text{v}} L_{\text{v}}} \tag{1}$$

In the case of highly wetting fluids, the order of magnitude of the superheat necessary to initiate boiling is about 10°. For such a superheat, one must take into account the non-linearity of the saturation curve and the variation of surface tension with temperature, using for example, a Van der Walls–Guggenheim law [6,8]. Eq. (1) becomes:

$$\exp\left[A - \frac{B}{T_{\text{w}} + C}\right] - P_{\text{l}} = \frac{2\sigma_0}{r_{\text{c}}} \left(1 - \frac{T_{\text{w}}}{T_{\text{c}}}\right)^{\mu} \tag{2}$$

where T_{c} is the thermodynamic critical temperature (469.4 K for *n*-pentane). Superheat and contact angle (through r_{c} and indirectly σ) determine thus the volume of the vapor embryo that grows in relation with the increase of the wall temperature. Eq. (2) was used to evaluate the critical radius corresponding to experimental superheat. The following coefficients were reported for *n*-pentane: $A = 20.73$, $B = 2477.07$ K, $C = -39.94$ K, $\sigma_0 = 52.34 \times 10^{-3}$ N m^{-1} and $\mu = 1.21$ [25].

The critical radius r_{c}, value of r_{b} for which the bubble growth is spontaneous, could be determined from the stability criterion of Mitzukami [24]:

$$\frac{\text{d}}{\text{d}V_{\text{b}}}\left(\frac{1}{r_{\text{b}}}\right) < 0 \tag{3}$$

The critical superheat is determined by taking into account the thermophysical properties of the fluid and the microgeometry of the boiling surface: Eq. (3) associated with (2) permit to evaluate the theoretical boiling superheat corresponding to a given shape of a cavity and a given contact angle. In the case of highly wetting liquids, for a conical shape cavity, Tong et al. [6] reported that $r_{\text{c}} < r_{\text{p}}$. Thormalhen [24], in the case of spherical cavity, demonstrated that $r_{\text{c}} \approx r_{\text{p}}$. If the surface is smooth the superheat could be large: if the cavities are too open, the liquid floods them and the sites cannot be activated. Indeed, considering an idealized conical cavity with a cone angle 2Φ and a mouth radius r_{p}, a liquid film flows into the cavity with a dynamic angle β_{d}, the trapping criteria of Bankoff said that vapor is trapped in the cavity if $\beta_{\text{d}} > 2\Phi$. As a consequence, a range of active cavity size exists for each combination of surface material, geometry, liquid, superheat and "flooding conditions".

Eq. (2) was used to determine the critical embryonic bubble radius corresponding to our experimental superheat values. The extreme value of boiling incipience superheat observed on the cylinder alone (the polished surface and the lateral face) ranged from 10.7 to 30.5 K, the corresponding values of the critical radius ranged from 0.14 to 0.61 μm. This order of magnitude was compatible with the size of the metal asperities measured, after the tests, with an interferometric rugosimeter. The r_{c} values related with the mean values of $\Delta T_{\text{sat}\,i}$ (group 3 in Fig. 9) ranged from 0.17 to 0.36 μm.

For group 2, $\Delta T_{\text{sat}\,i}$ ranged from 0.4 to 6.6 K, the corresponding critical embryonic bubble radius in the

porous medium have been calculated and ranged from 1.1 to 20.3 μm. The range of these values correspond to the range of pore diameters measured by mercury porosimetry (0.9–25.8 μm). Note that these values correspond to a cylinder superheat i.e. that the superheats on the porous were lower and then critical radius were underestimate. Microstructure of sintered Pyrex material might form a large number of cavities and the pores could be approximated as in spherical shape (Fig. 4). This type of cavity geometry has good vapor entrapment and stability. Moreover, in this case, the critical radius is essentially the mouth radius. Evaluation of $\Delta T_{\mathrm{sat}\,i}$ is possible for this porous disk directly by measuring the size distribution of the pores.

In order to find the value of $\Delta T_{\mathrm{sat}\,i}$ on the porous disk the system was modeled by a one-dimensional, multilayer, semi-infinite domain, for which the energy balance equation was numerically solved using the thermal quadrupoles method [26,27] (see Appendix A).

The numerical model was able to predict the temperature evolution anywhere in each layer for a given heat flux and with a realistic assumption on $\Delta T_{\mathrm{sat}\,i}$ of the cylinder and of the porous medium it was able to determine the threshold value of the confinement as a function of heat flux. The calculated threshold values of e ranged from 1000 to 2000 μm for heat flux steps ranging from 50 to 200 $\mathrm{kW\,m^{-2}}$ i.e. numerical results were one order of magnitude greater than the experimental ones. This result suggests that this purely conductive model ignores a determining physical phenomenon that tends, for a certain confinement value, to prevent heat transfer towards the porous medium. This mechanism seems to be due to two- or three-dimensional convective flows inside the spacing, which seem unusual, considering the aspect ratio e/r_{cyl} of the confined zone. No clear explanation for this difference was found, the origin might be linked with the complex flow and heat transfer in the vicinity of the liquid meniscus around the heated cylinder. For example, when the cylinder reached a temperature ranging from 40 to 45 °C, pulsated downwards jets, regularly located along the meniscus, were observed coming from the three-phase line (Fig. 10). Jet frequency ranged from 0.3 to 0.4 Hz. Despite of its simplicity, this numerical model justified the notion of threshold thickness value highlighted by the experiments.

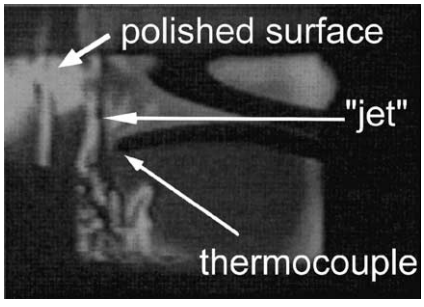

Fig. 10. View of the lateral jets around the cylinder (right).

5. Conclusions

The phenomena associated with boiling incipience of a highly wetting liquid in horizontal confined space with 30 mm diameter and a height ranging from 0 to 240 μm has been explored. This confinement zone was located between a polished face of a heated cylinder and a plain or porous disk. In the configuration studied, boiling incipience with *n*-pentane occurs during transient evolution consecutively of the application, on the upper face of the cylinder, of a heat flux step ranging between 50 and 200 $\mathrm{kW\,m^{-2}}$.

In the configuration with a plain disk, the influence of the height of the confined zone was not clearly shown. Boiling incipience superheat ranged from 16.1 to 27.2 °C, corresponding to the critical bubble radius ranging from 0.17 to 0.36 μm, values compatible with the surface defects of the polish cylinder face.

In the configuration with the porous disk, the height was a determinant parameter on boiling incipience. When the porous disk was far away from the polished surface, the boiling incipience superheat values were quite the same as in the plain-disk configuration. When the distance was lower than 100 μm, the superheat decreased drastically, ranging between 0.4 and 6.6 °C, corresponding with a critical bubble radius ranging from 1.1 to 20.3 μm. In this case, boiling appeared on the porous disk, in which cavities of this size were in this range.

Heat transfer controlled boiling incipience on the porous surface in the liquid layer. For a given heat flux, a threshold value e_{thr} exists. Due to the random behavior of the boiling incipience phenomena, in our experimental results, this threshold appears as a transition range. In this range of confined space height, boiling could appear randomly on the heated or the non-heated surface, with a high or a low cylinder superheat.

Appendix A. Modelization of the system temperature evolution with thermal quadrupole method

The test configuration was modeled using the thermal quadrupoles method [26,27]. This method is particularly adapted to solve unsteady pure conductive problems in the case of multilayer material. The experimental configuration was modeled by six layers: heating element and PTFE insulation (0), cylinder thickness with shoulder (1), straight part of cylinder (2), liquid layer (3), confinement disk (4) and liquid pool (5).

The following assumptions have been made: the heat transfer problem was one-dimensional ($Bi \approx 0.014$) in the cylinder, experimental temperature differences ($T_2 - T_{lat}$), measured between the center and the periphery, in the period preceding incipience, were of the same order of magnitude as the uncertainty on ΔT. Only conductive thermal transfers were considered in the cylinder: heat flux associated with liquid vaporization in the meniscus was assumed negligible. In the confinement zone, upward heating, aspect ratio e/D greater than 150 and the position of the pool liquid level lower than the polished surface, expected to take into account conductive thermal transfer in the liquid layer. Thermal resistance in the interface with liquid was neglected, and the physical properties of material were assumed to be constant. In the layer (1) the Cp was increased to take into account section variation and in the layer (3) the effective thermal conductivity of the porous media was calculated using a parallel mixture law. Lateral faces were considered as adiabatic and the liquid pool as a semi-infinite domain.

Initially at constant temperature (T_{sat}), at instant t_0 the system was submitted to a heat flux step q_0 on the upper face of layer (0). In the real system a part of the energy is lost to the thermal capacity of the upper insulation material. In the contact area between the heating element and the cylinder; thermal resistances existed and were expected to vary with the dilatation of the different elements, thermophysical properties of the heating element could also vary with important temperature changes. To take into account of this non-linearity, the thermal diffusivity of the heating element was considered as a function of heat flux. This empirical law and the thermal diffusivity of the cylinder were fitted with experimental data using a least squares method on four cases tested for a configuration without confinement disk.

A.1. Model description

The energy equation for an homogenous, 1D, isotropic wall, with a thickness e, $T(x,0) = 0$ and constant thermophysical properties is:

$$\frac{\partial T}{\partial t} = a\frac{\partial^2 T}{\partial x^2} \tag{A.1}$$

Laplace transformation applied to the energy equation, with $L[T(x,t)] = \theta(x,p)$ gives:

$$\frac{p}{a}\theta = \frac{\mathrm{d}^2\theta}{\mathrm{d}x^2} \tag{A.2}$$

Solving this equation permit to express the solution in the Laplace space as a matrix with θ_e, θ_s, respectively input and output temperature, and Φ_e, Φ_s, respectively input and output heat flux [26]:

$$\begin{bmatrix} \theta_e \\ \Phi_e \end{bmatrix} = \begin{bmatrix} \mathrm{ch}(\alpha\sqrt{p}) & \frac{\beta}{\sqrt{p}}\,\mathrm{sh}(\alpha\sqrt{p}) \\ \gamma\sqrt{p}\,\mathrm{sh}(\alpha\sqrt{p}) & \mathrm{ch}(\alpha\sqrt{p}) \end{bmatrix} \begin{bmatrix} \theta_s \\ \Phi_s \end{bmatrix} \tag{A.3}$$

with

$$\alpha = \frac{e}{\sqrt{a}}, \quad \beta = \frac{\sqrt{a}}{\lambda} \quad \text{and} \quad \gamma = \frac{1}{\beta}$$

The experimental system, modeled as a multilayer one-dimensional material, was described in the thermal quadrupoles formalism, by multiplication of five transfer matrix corresponding to each layer: [A_0] the heating element, [A_1] cylinder shoulder, [A_2] cylinder straight part, [A_3] confinement zone with liquid ($e_3 = e$), [A_4] confinement wall.

Boundary conditions:

1. Constant heat flux q_0 (Neumann), on one wall face, the inlet vector becomes:

$$\begin{bmatrix} \theta_{0e} \\ \Phi_{0e} \end{bmatrix} = \begin{bmatrix} \theta_{0e} \\ \frac{q_0}{p} \end{bmatrix} \tag{A.4}$$

2. Semi-infinite domain, the inlet vector becomes:

$$\begin{bmatrix} \theta_{5e} \\ \Phi_{5e} \end{bmatrix} = \begin{bmatrix} \theta_s \\ \gamma_5\Phi_s \end{bmatrix} \tag{A.5}$$

System resolution, by multiplying and inverting matrices, gives $\theta(x,p)$ and the Gaver–Stehfest method is used to find the numerical solution $T(x,t)$ from $\theta(x,p)$.

References

[1] J. Ku, Recent advances in capillary pumped loop technology, in: Proceedings AIAA Nat. Heat Transfer Conf., Baltimore, Maryland, August, 97-3870, 1997, pp. 1–21.

[2] B. Cullimore, Start up transient in capillary pumped loops, AIAA Paper No. 91-1374, 1991.

[3] V. Dupont, V. Platel, J.L. Joly, C. Butto, Capillary pumped loop startup: effects of the wick fit in the evaporator, in: Proceedings 19th AIAA Conf., Toulouse, 17–20 April, 2001.

[4] J.G. Collier, J.R. Thome, Convective Boiling and Condensation, Oxford Science Publications, Oxford, 1994.

[5] A. Bar-Cohen, T.W. Simon, Wall superheat excursions in the boiling incipience of dielectric, Heat Transfer Eng. 9 (3) (1988) 19–30.

[6] W. Tong, A. Bar-Cohen, T.W. Simon, S.M. You, Contact angle effect on boiling incipience of highly-wetting liquids, Int. J. Heat Mass Transfer 33 (1) (1990) 91–103.

[7] S.M. You, T.W. Simon, A. Bar-Cohen, W. Tong, Experimental investigation of nucleate boiling incipience with a highly-wetting dielectric fluid (R-113), Int. J. Heat Mass Transfer 33 (1) (1990) 105–117.

[8] S.M. You, A. Bar-Cohen, T.W. Simon, Boiling incipience and nucleate boiling heat transfer of highly-wetting dielectric fluids from electronic materials, IEEE Trans. 13 (4) (1990) 1032–1039.

[9] A.E. Bergles, Enhancement of pool boiling, Int. J. Refrig. 8 (20) (1997) 545–551.
[10] N.H. Afgan, L.A. Jovic, S.A. Kovalev, V.A. Lenykov, Boiling heat transfer from surfaces with porous layers, Int. J. Heat Mass Transfer 40 (1985) 415–422.
[11] J. Tehver, H. Sui, V. Temkina, Heat transfer and hysteresis phenomena in boiling on porous plasma-sprayed surface, Exp. Thermal Fluid Sci. 5 (1992) 714–727.
[12] J.Y. Chang, S.M. You, Enhanced boiling heat transfer from micro porous surfaces: effect of a coating composition and method, Int. J. Heat Mass Transfer 40 (18) (1997) 4449–4460.
[13] H.S. Liang, W.J. Yang, A remedy for hysteresis in nucleate boiling trough application of micrographite-fiber nucleation activators, Exp. Heat Transfer (9) (1996) 323–334.
[14] H.S. Liang, W.J. Yang, Nucleate pool boiling heat transfer in a highly-wetting liquid on micro-graphite-fiber composite surfaces, Int. J. Heat Mass Transfer 41 (13) (1998) 1993–2001.
[15] J.R. Thome, Enhanced Boiling Heat Transfer, Hemisphere Pub. Corp, 1990.
[16] S.J. Reed, I. Mudawar, Elimination of boiling incipience temperature drop in highly-wetting fluids using spherical contact with a flat surface, Int. J. Heat Mass Transfer 42 (1999) 2439–2454.
[17] A. Faghri, Heat Pipe Science and Technology, Taylor and Francis, Washington, 1995.
[18] S.M. You, T.W. Simon, A. Bar-Cohen, Y.S. Hong, Effect of dissolved gas content on pool boiling of a highly-wetting fluid, J. Heat Transfer 117 (1995) 687–692.
[19] K. Moriyama, A. Inoue, Thickness of the liquid film formed by a growing bubble in a narrow gap between two horizontal plates, J. Heat Transfer 118 (1996) 132–139.
[20] V. Dupont, Etude expérimentale du déclenchement de l'ébullition en milieu confiné horizontal: application à l'amorçage des boucles fluides diphasiques à pompage thermocapillaire, Ph.D. Thesis, Université Paul Sabatier, Toulouse, France, 2001.
[21] A. Moffat, Describing the uncertainties in experimental results, Exp. Thermal Fluid Sci. (1988) 3–17.
[22] J.H. Lienhard, A.H. Karimi, Corresponding state correlations of the extreme liquid superheat and vapour subcooling, J. Heat Transfer 100 (1978) 492–495.
[23] X.F. Peng, D. Liu, D.J. Lee, Y. Yan, B.X. Wang, Cluster dynamics and fictitious boiling in microchannels, Int. J. Heat Mass Transfer 43 (2000) 4259–4265.
[24] I. Thormählen, Superheating of liquids at the onset of boiling, in: Proceedings 8th Int. Heat Transfer Conf. (4), San Francisco, 1986, pp. 2001–2006.
[25] I.A McLure, V.A.M. Soares, B. Emonds, Surface tension of perfluoropropane, perfluoro-*n*-butane, perfluoro-*n*-hexane, perfluorotributylamine and *n*-pentane, J. Chem. Soc. Faraday Trans. 1 (78) (1982) 251–257.
[26] A. Degiovanni, Conduction dans un "mur" multicouche avec sources: extension à la notion de quadripôle, Int. J. Heat Mass Transfer 31 (3) (1988) 553–557.
[27] D. Maillet, S. André, J.C. Batsale, A. Degiovanni, C. Moyne, Thermal Quadrupoles, first ed., Wiley, Chichester, 2000, pp. 342–355.